

Thermodynamic Generalized Compressibility in a Glass Forming Liquid

Hervé M. Carruzzo and Clare C. Yu

Department of Physics and Astronomy, University of California, Irvine, Irvine, California 92697
(February 5, 2020)

We introduce a new thermodynamic quantity to probe the glass transition. This quantity is a linear generalized compressibility which depends solely on the positions of the particles. We have performed a molecular dynamics simulation on a glass forming liquid consisting of a two component mixture of soft spheres in three dimensions. As the temperature is lowered, the generalized compressibility drops sharply at the glass transition. Our results support both a random first order transition and the kinetic view of the glass transition.

The glass transition is still not well understood despite extensive study. It is characterized by both kinetic and thermodynamic features. For example in the supercooled liquid kinetic quantities such as the viscosity and relaxation time grow rapidly as the temperature is lowered. The glass transition is reflected in thermodynamic quantities such as the specific heat which has a step-like form and in the dielectric constant which exhibits a peak whose position is frequency dependent.

There have been two main theoretical approaches to the problem: dynamic and thermodynamic. Theories in the first category view the glass transition as a kinetic phenomenon characterized by a growing relaxation time and viscosity [1–5]. When the relaxation time exceeds the measurement time, particle motion appears to be arrested resulting in the glass transition. Interesting and fruitful concepts such as the influence of the energy landscape on relaxation processes [6,7] and dynamic inhomogeneities [4,8,9] have resulted from this approach. The thermodynamic viewpoint attributes the glass transition to an underlying phase transition hidden from direct experimental observation by extremely long relaxation times [1,2,10–12]. In most scenarios there is an underlying second order phase transition associated with a growing correlation length which produces diverging relaxation times as well as diverging static susceptibilities [13–18]. More recently Mezard and Parisi [12] have argued that the underlying transition is actually a random first order transition signaled by a discontinuity in the specific heat.

In an effort to better characterize the glass transition we introduce a novel thermodynamic probe which we call a generalized compressibility [19]. Unlike the specific heat which monitors energy fluctuations, this linear compressibility is a function of the microscopic structure of the system: it depends solely on the positions of the particles and not on their previous history. It is easy to compute numerically, and it is simpler than the dielectric constant which involves both the translation and orientation of electric dipoles. Our generalized compressibility should be directly measurable experimentally in

colloidal suspensions of polystyrene spheres [20] and possibly in other systems as well. In this paper we present measurements of this quantity in a molecular dynamics simulation of a two component system of soft spheres. We find that the linear generalized compressibility drops sharply as the temperature decreases below the glass transition temperature T_g . The drop becomes more and more abrupt as the measurement time increases.

We now derive expressions for the linear and nonlinear generalized compressibility. To probe the density fluctuations, we follow the approach of linear response theory and consider applying an external potential $\frac{\Delta P}{\rho_o} \phi(\vec{r})$ which couples to the local density $\rho(\vec{r}) = \sum_{i=1}^N \delta(\vec{r} - \vec{r}_i)$ where \vec{r}_i denotes the position of the i^{th} particle. ρ_o is the average density. ΔP has units of pressure and sets the magnitude of the perturbation. $\phi(\vec{r})$ is a dimensionless function of position that must be compatible with the periodic boundary conditions imposed on the system, i.e., it must be continuous across the boundaries, but is otherwise arbitrary. This adds to the Hamiltonian H of the system a term

$$U = \frac{\Delta P}{\rho_o} \int_V dr^3 \phi(\vec{r}) \rho(\vec{r}) = \frac{\Delta P}{\rho_o} \sum_i \phi(\vec{r}_i) \equiv \frac{\Delta P}{\rho_o} \rho_\phi \quad (1)$$

where we have defined $\rho_\phi = \int_V dr^3 \phi(\vec{r}) \rho(\vec{r}) = \sum_i \phi(\vec{r}_i)$. ρ_ϕ is the inner product of ϕ and $\rho(\vec{r})$, and we can regard it as a projection of the density onto a basis function $\phi(r)$, i.e., $\rho_\phi = \langle \rho | \phi \rangle$. It weights the density fluctuations according to their spatial position. The application of the external potential will induce an average change $\delta \rho_\phi$ in ρ_ϕ :

$$\delta \rho_\phi = \frac{1}{\rho_o N} \{ \langle \rho_\phi \rangle_U - \langle \rho_\phi \rangle_{U=0} \} \quad (2)$$

where the thermal average $\langle \rho_\phi \rangle_U$ is given by

$$\langle \rho_\phi \rangle_U = \frac{1}{\mathcal{Z}} \text{Tr} \left[e^{-\beta(H+U)} \rho_\phi \right] \quad (3)$$

The partition function $\mathcal{Z} = \text{Tr} e^{-\beta(H+U)}$ and β is the inverse temperature. For small values of ΔP , this change

can be calculated using perturbation theory. Up to third order in ΔP , we find

$$\begin{aligned}\delta\rho_\phi = \beta \frac{\Delta P}{\rho_o} \langle \rho_\phi^2 \rangle_c - \frac{\beta^2 \Delta P^2}{2\rho_o^2} \langle \rho_\phi^3 \rangle_c \\ + \frac{\beta^3 \Delta P^3}{6\rho_o^3} \langle \rho_\phi^4 \rangle_c,\end{aligned}\quad (4)$$

where the cumulant averages are

$$\langle \rho_\phi^2 \rangle_c = \langle \rho_\phi^2 \rangle - \langle \rho_\phi \rangle^2 \quad (5)$$

$$\langle \rho_\phi^3 \rangle_c = \langle \rho_\phi^3 \rangle - 3\langle \rho_\phi \rangle \langle \rho_\phi^2 \rangle + 2\langle \rho_\phi \rangle^3 \quad (6)$$

$$\begin{aligned}\langle \rho_\phi^4 \rangle_c = \langle \rho_\phi^4 \rangle - 4\langle \rho_\phi \rangle \langle \rho_\phi^3 \rangle - 3\langle \rho_\phi^2 \rangle^2 + \\ 12\langle \rho_\phi \rangle^2 \langle \rho_\phi^2 \rangle - 6\langle \rho_\phi \rangle^4\end{aligned}\quad (7)$$

with the thermal average $\langle \rho_\phi^n \rangle = \langle \rho_\phi^n \rangle_{U=0}$. The third order cumulant, eq.(6), is zero in the liquid phase because for every configuration there exists an equivalent configuration with the opposite sign of $\rho_\phi - \langle \rho_\phi \rangle$ and so we will not consider this term any further. We can recast eq. (4) as a power series in the perturbation ΔP :

$$\frac{\langle \delta\rho_\phi \rangle}{\rho_o N} = \frac{1}{2\rho_o T} \chi_l \Delta P - \frac{1}{2(\rho_o T)^3} \chi_{nl} (\Delta P)^3 \quad (8)$$

where

$$\chi_l = \frac{2d}{N} \langle (\rho_\phi)^2 \rangle_c \quad \chi_{nl} = -\frac{d}{3N} \langle (\rho_\phi)^4 \rangle_c. \quad (9)$$

d is the dimension of the system. In the remainder of this paper we will focus our attention on the linear (χ_l) and nonlinear (χ_{nl}) dimensionless generalized compressibilities defined by the above expressions. We now discuss the choice of the function ϕ . We consider applying the potential along the direction μ of one of the coordinate axes so that $\phi(\vec{r}) = \phi(r^\mu)$. A natural candidate for $\phi(r^\mu)$ is $\cos(k_\mu r^\mu)$ with $k = 2\pi n/L$, where $n = 1, 2, \dots$ and L^3 is the volume V . In this case, ρ_ϕ is the k^{th} mode of the cosine transform of the density. However, it is sufficient to consider the simpler function $\phi(r^\mu) = |r^\mu|/L$. The absolute value corresponds to the case where all the particles feel a force along the μ th direction pointing towards the origin. It gives results very similar to $\phi(r^\mu) = \cos(k_\mu r^\mu)$ for small k at a fraction of the computational cost. So our results in this paper correspond to $\rho_\phi = \sum_i |r_i^\mu|/L$. This is rather like a center of mass. Since the system is isotropic, we average over the direction μ .

We have performed a molecular dynamics simulation on a glass forming liquid [21,22] consisting of a 50:50 binary mixture of soft spheres in three dimensions. The two types of spheres, labelled A and B, differ only in their sizes. The interaction between two particles a distance r apart is given by $V_{\alpha\beta}(r) = \epsilon[(\sigma_{\alpha\beta}/r)^{12} + X_{\alpha\beta}(r)]$ where the interaction length $\sigma_{\alpha\beta} = (\sigma_\alpha + \sigma_\beta)/2$, $\sigma_B/\sigma_A = 1.4$ ($\alpha, \beta = A, B$). For numerical efficiency, we set the cutoff function $X_{\alpha\beta}(r) = r/\sigma_{\alpha\beta} - \lambda$ with $\lambda = 13/12^{12/13}$.

The interaction is cutoff at the minimum of the potential $V_{\alpha\beta}(r)$. Energy and length are measured in units of ϵ and σ_A , respectively. Temperature is given in units of ϵ/k_B where k_B is Boltzmann's constant, and time is in units of $\sigma_A \sqrt{m/\epsilon}$ where m , the mass of the particles, is set to unity. The equations of motion were integrated using the leapfrog method [23] with a time step of 0.005. During each run the density $\rho_o = N/L^3$ and temperature were kept constant using a constraint algorithm [23]. $N = N_A + N_B$ is the total number of particles. The system occupies a cube with dimensions $(\pm L/2, \pm L/2, \pm L/2)$ and periodic boundary conditions.

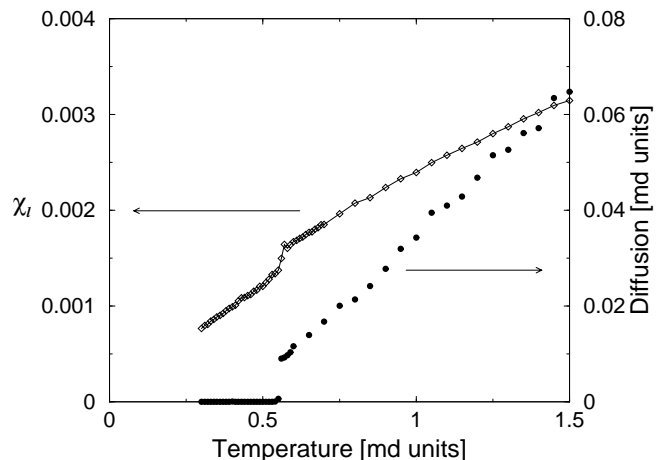


FIG. 1. Linear generalized compressibility and diffusion constant of a one component system as a function of temperature for 512 soft spheres. The crystalline behavior is clearly seen around $T=0.57$ ($\rho_o = 1.1$). The measurement time was 10^6 md steps for each temperature. The compressibility was averaged over 5 runs while the diffusion is shown for a single run.

The measuring procedure is as follows. We start each run at a high temperature ($T=1.5$) and lower the temperature in steps of $\Delta T = 0.05$. At each temperature we equilibrate for 10^4 molecular dynamics steps (md steps) and then measure the quantities of interest for N_τ additional md steps where $N_\tau = 10^5, 2 \times 10^5, 10^6$, or 3×10^6 . All the particles move at each md step. The results are then averaged over up to 40 different initial conditions (different initial positions and velocities of the spheres). As a check on our procedure for measuring χ_l and χ_{nl} , we consider first the case of the crystal. To this end, we consider a system of 512 identical ($\sigma_A = \sigma_B$) particles at a density $\rho_o = 1.1$.

Figure 1 shows the linear compressibility and the diffusion constant as a function of temperature for the single component liquid. At high temperatures χ_l has a small slope which becomes steeper at low temperature. The salient feature is the very sharp drop around $T=0.57$ of the linear generalized compressibility and the diffusion constant. The specific heat, which is not shown, has

a sharp delta function-like peak around $T=0.57$. The low temperature phase ($T<0.57$) is a crystal with sharp Bragg peaks in the structure factor. Upon heating and cooling, the transition shows hysteresis. All these observations are consistent with the fact that crystallization is a first order transition. Not shown here is the nonlinear compressibility which is zero within our numerical error.

We now examine the response of the two component glass forming liquid. All the runs were done at a density of $\rho_o = 0.6$ and $\sigma_B/\sigma_A = 1.4$. For these parameters crystallization is avoided upon cooling.

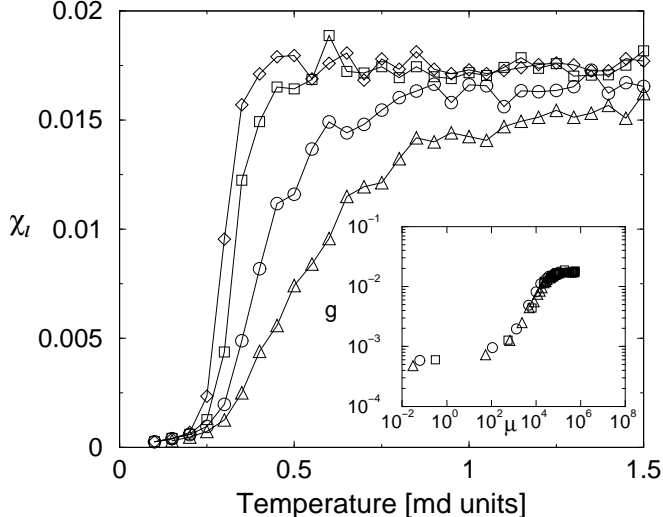


FIG. 2. Linear generalized compressibility as a function of temperature for different measuring times t_M : 10^5 (\triangle , 40 runs), 2×10^5 (\circ , 32 runs), 10^6 (\square , 10 runs) and 3×10^6 (\diamond , 6 runs) md steps. System size is 512 particles. $\rho_o = 0.6$ and $\sigma_B/\sigma_A = 1.4$. Inset: $T > T_o$ subset of the same data scaled as described in text.

Figure 2 shows the linear generalized compressibility as a function of temperature for different run times. The compressibility at high temperatures is independent of T and about an order of magnitude larger than that of the single component fluid. In the vicinity of the glass transition χ_l drops. Notice that as the measuring time t_M increases, the temperature of the drop decreases and becomes more abrupt. The linear compressibility is proportional to the width of the distribution of ρ_ϕ . If we regard ρ_ϕ as a generalized center of mass, then the drop in χ_l corresponds to the sudden narrowing of the distribution $P(\rho_\phi)$ and the sudden arrest in the fluctuations of ρ_ϕ . This behavior can be quantified using a scaling ansatz: $\chi_l(t_M, T) = g(\mu = t_M/\tau(T))$, where the characteristic time has the Volgel-Fulcher form $\tau(T) = \exp(A/(T - T_o))$. The inset of Figure 2 shows that the data collapse onto a single curve with $A = 0.75$, $T_o = 0.15$. (The data could not be fitted using $\tau(T) = A(T - T_o)^\gamma$ as suggested by simple mode coupling theories [3].) This scaling suggests that χ_l becomes a step function for infinite t_M and that the drop in

the compressibility would become a discontinuity at infinitely long times, in agreement with Mezard and Parisi's proposal that the glass transition is a first order phase transition [12]. The abrupt drop is also consistent with a sudden arrest of the motion of the particles in the liquid which is the kinetic view of the glass transition.

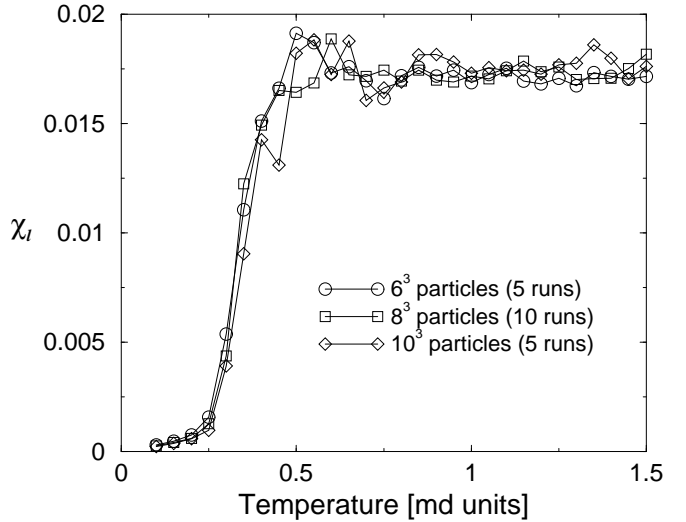


FIG. 3. Linear compressibility as a function of temperature for different system sizes: 216, 512 and 1000 particles. The measuring time was 10^6 md steps in all cases. Other parameters are the same as in Figure 2.

The behavior seen in Figure 2 is similar to that seen in measurements of the real part of the frequency dependent dielectric function $\varepsilon'(\omega)$ [18]. In that case as the frequency decreased, the temperature of the peak in $\varepsilon'(\omega)$ decreased and the drop in $\varepsilon'(\omega)$ below the peak became more abrupt. By extrapolating their data to $\omega = 0$, Menon and Nagel [18] argued that $\varepsilon'(\omega = 0)$ should diverge at the glass transition, signaling a second order phase transition. We have looked for evidence of this divergence by examining samples of different sizes to see if the linear generalized compressibility increased systematically with system size. As shown in Figure 3 we find no size dependence and no indication of a diverging linear generalized compressibility.

So far we have shown the results of cooling the system. In order to look for hysteretic behavior we have done runs in which we heat a system of 512 particles by starting at our lowest temperature $T = 0.1$ with a configuration obtained by cooling the system. We then increased the temperature in steps of $\Delta T = 0.05$. As before we equilibrate at each temperature for 10^4 time steps and then measure quantities for an additional 10^6 time steps. Our results are shown in Figure 4. Notice the slight hysteresis with the rise in χ_l upon warming being at a slightly higher temperature than the drop in χ_l upon cooling. This hysteresis is consistent with both views of the glass transition, i.e., the kinetic arrest of motion and

the random first order phase transition.

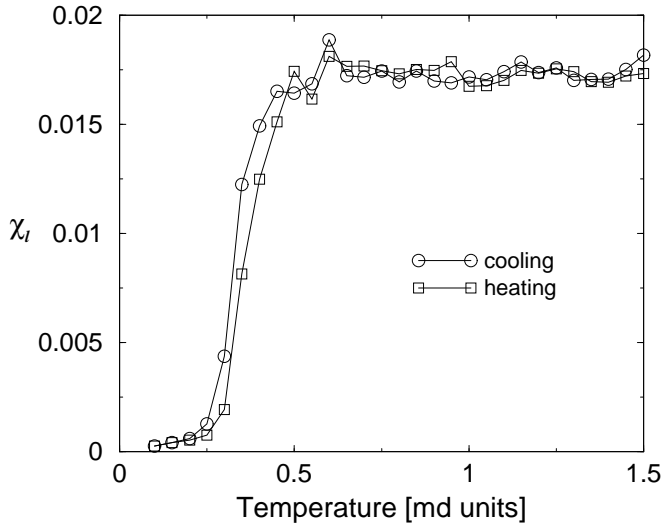


FIG. 4. Linear generalized compressibility as a function of temperature for system of 512 particles upon cooling and heating. The measuring time was 10^6 md steps in both cases. The data was averaged over 10 runs. Other parameters are the same as in Figure 2.

We now turn to the case of the nonlinear generalized compressibility χ_{nl} given by eq. (9). We are motivated by the case of spin glasses where the nonlinear magnetic compressibility diverges at the spin glass transition while the linear compressibility only has a cusp [24,25]. There have been a few studies of nonlinear response functions in real glasses [17,26], but these have not found any divergences. Our results are consistent with this conclusion. In particular we find that the nonlinear generalized compressibility is zero above and below the glass transition temperature, though it does show a glitch at the glass transition. There is no systematic increase with system size, indicating the absence of a divergence. Because χ_{nl} is sensitive to the tails of the distribution of ρ_ϕ , one must be careful to obtain a good ensemble average in the liquid above the glass transition temperature. We have done this by doing 32 runs, each involving 200,000 time steps, with different initial conditions, stringing them together as though they were one long run and then taking the appropriate averages. This produces a better ensemble average of $\langle \rho_\phi^2 \rangle^2$ which enters into χ_{nl} in eq. (6). χ_{nl} also took longer to equilibrate than χ_l . By plotting χ_{nl} versus run time, we found that one had to run at least 10^6 time steps before χ_{nl} appeared to saturate.

To summarize, we have introduced a new thermodynamic quantity which depends solely on the positions of the particles and not on their histories. This quantity drops abruptly at the glass transition. Its behavior is compatible with both a random first order transition and a kinetic arrest of motion, but not with an underlying second order phase transition. This generalized com-

pressibility can be experimentally measured in several ways. It can be directly measured in colloidal experiments which monitor the positions of the particles. One can also put a glass forming liquid in a centrifuge and plot the density as a function of rate of rotation. The slope is the linear generalized compressibility. This slope should change abruptly at the glass transition. Measurements of the width of the distribution of ρ_q , the spatial Fourier transform of the density, would also give the linear generalized compressibility.

We thank Andrea Liu for helpful discussions. This work was supported in part by CULAR funds provided by the University of California for the conduct of discretionary research by Los Alamos National Laboratory.

- [1] M. D. Ediger, C. A. Angell, and S. R. Nagel, *J. Phys. Chem* **100**, 13200 (1996), and references therein.
- [2] J. T. Fourkas, D. Kivelson, U. Mohanty, and K. A. Nelson, *Supercooled Liquids: Advances and Novel Applications* (American Chemical Society, Washington, D. C., 1997).
- [3] W. Götze and L. Sjögren, *Rep. Prog. Phys.* **55**, 241 (1992).
- [4] C. Donati *et al.*, *Phys. Rev. Lett.* **80**, 2338 (1998).
- [5] R. Yamamoto and A. Onuki, *Europhys. Lett.* **40**, 61 (1997).
- [6] M. Goldstein, *J. Chem. Phys.* **51**, 3728 (1969).
- [7] S. Sastry, P. G. Debenedetti, and F. H. Stillinger, *Nature* **393**, 554 (1998).
- [8] R. Yamamoto and A. Onuki, *J. Phys. Soc. (Japan)* **66**, 2545 (1997).
- [9] U. Tracht *et al.*, *Phys. Rev. Lett.* **81**, 2727 (1998).
- [10] G. Adam and J. H. Gibbs, *J. Chem. Phys.* **43**, 139 (1965).
- [11] J. H. Gibbs and E. A. DiMarzio, *J. Chem. Phys.* **28**, 373 (1958).
- [12] M. Mézard and G. Parisi, *Phys. Rev. Lett.* **82**, 747 (1999).
- [13] T. R. Kirkpatrick, D. Thirumalai, and P. G. Wolynes, *Phys. Rev. A* **40**, 1045 (1989).
- [14] J. P. Sethna, J. D. Shore, and M. Huang, *Phys. Rev. B* **44**, 4943 (1991).
- [15] D. Kivelson *et al.*, *Physica A* **219**, 27 (1995).
- [16] R. M. Ernst, S. R. Nagel, and G. S. Grest, *Phys. Rev. B* **43**, 8070 (1991).
- [17] C. Dasgupta, A. V. Indrani, S. Ramaswamy, and M. K. Phani, *Europhys. Lett.* **15**, 307 (1991).
- [18] N. Menon and S. R. Nagel, *Phys. Rev. Lett.* **74**, 1230 (1995).
- [19] J. Yvon, *Suppl. Nuovo Cim.* **9**, 144 (1958).
- [20] E. R. Weeks *et al.*, *Science* **287**, 627 (2000).
- [21] T. A. Weber and F. H. Stillinger, *Phys. Rev. B* **31**, 1954 (1985).
- [22] W. Kob and H. C. Andersen, *Phys. Rev. Lett.* **73**, 1376 (1994).

- [23] D. C. Rapaport, *The art of molecular dynamics simulation* (Cambridge University Press, New York, 1995).
- [24] R. N. Bhatt and A. P. Young, Phys. Rev. B **37**, 5606 (1988).
- [25] L. P. Levy and A. T. Ogielski, Phys. Rev. Lett. **57**, 3288 (1986).
- [26] L. Wu, Phys. Rev. B **43**, 9906 (1991).